Using ODGWs with GSAOI: Software and Firmware Implementation Challenges

Peter J. Young*[a], Peter McGregor[a], Jan van Harmelen[a], Benoît Neichel[b]
[a]Research School of Astronomy & Astrophysics, College of Physical and Mathematical Sciences, The Australian National University, Cotter Road, ACT, Australia 2611;
[b]Gemini Observatory, Southern Operations Center, c/o AURA, Casilla 603, La Serena, Chile

ABSTRACT

The Gemini South Adaptive-Optics Imager (GSAOI) has recently been commissioned on the Gemini South telescope. Designed for use with the Gemini GeMS Multi-Conjugate Adaptive Optics System, GSAOI makes use of the HAWAII-2RG (H2RG) On-Detector Guide Window (ODGW) feature where guide windows positioned in each of the four H2RG detectors provide GeMS with tip-tilt and flexure corrections. This paper concentrates on the complex software and firmware required for operating the ODGWs and for delivering the performance required by GeMS. Software architecture, algorithms, performance and the implementation platform for the current on-telescope solution are detailed.

Keywords: On-detector guide windows, multi-conjugate adaptive optics, GSAOI, GeMS, HAWAII-2RG

1. INTRODUCTION

The use of ODGWs as a feature of the Gemini GSAOI instrument was first reported at the SPIE conference in Glasgow in 2004 (McGregor et al., 2004). GSAOI was constructed by The Australian National University and delivered to the Gemini Observatory in 2006 but has since been in storage awaiting the arrival of the Gemini adaptive-optics system in 2010. During 2011 and 2012 these two instruments have been undergoing commissioning at Gemini South.

This paper describes the ODGW solution as implemented in GSAOI from a mainly software perspective. It is a complex system with many components in the end-to-end architecture.

2. GSAOI & GEMS ARCHITECTURE

2.1.1 GSAOI

As described by McGregor (2004)[2], GSAOI will be the workhorse instrument used with GeMS. GSAOI is a near-infrared, diffraction-limited, imaging system and uses a mosaic of HAWAII-2RG detectors with 4k×4k pixels arranged in four 2k×2k quadrants.

Any rectangular region of the four GSAOI H2RG detectors can be read out while the remainder of the array is integrating. These regions (i.e., ODGWs) are read out repeatedly during a science imager integration to monitor image translation for tip-tilt or flexure correction. In addition, while a full imager frame is being read out, ODGWs are sampled in an interleaved fashion to maintain corrections during science data gathering. This interleaving of ODGW data with science data is performed at a programmable integral number of full science row reads – thus compromising the ODGW delivery rate and also extending the full frame read time.

Centroids and image flux from each of the ODGWs are passed on to GeMS as a contribution to the overall adaptive optics solution (see §2.1.2). The data flow from detectors through SDSU electronics, GSAOI Detector Controller (DC), GeMS Real-Time Controller (RTC) and Adaptive-Optics Module (AOM) and finally the GeMS optical bench (Canopus) is shown in Figure 1.

2.1.2 GeMS

A schematic view of the main components of GeMS is shown in Figure 2 (See Neichel, 2010[3] and Rigaut, 2011[4]).

* pjy@mso.anu.edu.au; phone 61 2 612 50281; fax 61 2 612 50233; www.mso.anu.edu.au

Software and Cyberinfrastructure for Astronomy II, edited by Nicole M. Radziwill, Gianluca Chiozzi,
Proc. of SPIE Vol. 8451, 845124 · © 2012 SPIE · CCC code: 0277-786X/12/$18 · doi: 10.1117/12.925273

Downloaded From: http://proceedings.spiedigitallibrary.org/ on 04/08/2013 Terms of Use: http://spiedl.org/terms

GeMS uses five artificial laser guide stars (LGS) with their associated LGS wave-front sensors (LGS WFSs) and three deformable mirrors (DMs) to compensate the turbulence over a field of view of 2 arcmin in diameter. In addition, GeMS requires natural guide stars (NGSs) to compensate for tip-tilt and plate scale modes. Ideally, three guide stars should be available to compensate for tip-tilt and plate-dynamical errors. However GeMS may work with two or one tip-tilt NGSs with reduced performance. Tip-tilt control (i.e., fast tip-tilt guiding) can be performed at up to 800Hz. The NGSs are also used to compensate for the differential flexure between the adaptive-optics bench and GSAOI (i.e., flexure compensation) and for the slow variation of the sodium layer altitude (i.e., focus compensation). In these cases, a frame rate of only ~1Hz is required.

For fast tip-tilt guiding, the adaptive-optics bench contains three WFS probes, each containing a reflective pyramid that acts like a quad-cell feeding a set of four fibers and associated avalanche photodiodes. One of the probes also contains a small beam splitter that sends light to a 2×2 Shack-Hartmann WFS used to monitor slow focus variations. In this configuration, the science instrument provides an "on-instrument" guiding capability that is used only to compensate for differential flexure. This is called 3+1 mode, i.e., three visible fast tip-tilt NGS and one near-infrared flexure star.

In the case of GSAOI, a second mode of operation is allowed. Based on the unique capability of the ODGWs, the fast tip-tilt guiding can be provided directly by the instrument. The ODGWs are used in a fast readout mode, providing the tip-tilt information based on the centroid position of the stars. In this mode, one visible star is still used for slow focus compensation. This mode is called 1+3, i.e., one visible focus NGS and three fast TT near-infrared tip-tilt NGSs.

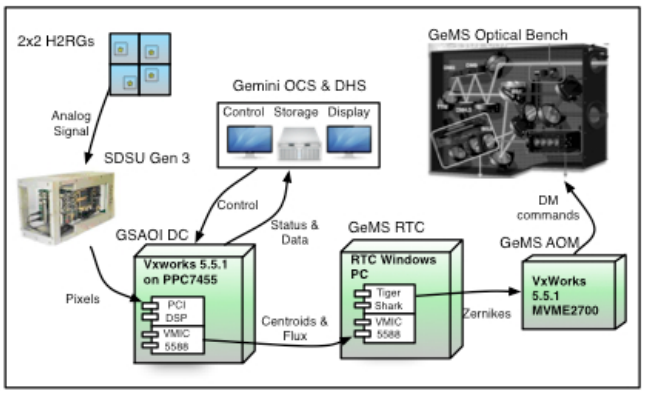

Figure 1: Data flow from H2RG ODGWs to GeMS optical bench

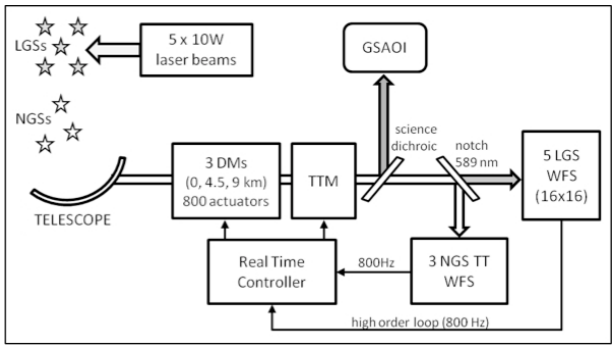

Figure 2: GeMS schematic view

3. CONCEPT OF OPERATION

The detailed operation of the ODGWs depends on the stage of the science image read out being executed. The ODGWs must be read out before the science exposure begins to allow the ODGW guide stars to be set up and the adaptive-optics control loops to be closed. The GSAOI science imager is regularly reset during this time in its "idle" mode, so ODGW reads must be interleaved with the resetting of blocks of science image rows (i.e., ODGW interleaved-idle mode; Figure 3). The ODGWs are not reset by the science image reset in this mode.

The current ODGW exposure is terminated asynchronously when a science exposure is initiated (Figure 4). ODGW reads must then continue at regular intervals to ensure that the adaptive-optics control loops stay closed. The science imager is first reset to begin the exposure sequence, so ODGW reads occur interleaved with blocks of these science row resets (i.e., ODGW interleaved-reset mode). It is unavoidable in the GSAOI system that the science image also asynchronously resets the ODGW in this mode. The ODGW exposure is labeled invalid when this occurs. The actual science exposure begins with the first set of Fowler Non-Destructive Reads (NDRs). The ODGW must be read prior to the commencement of these science NDRs in order to prevent cosmetic artifacts appearing in the science imager. This forced ODGW read truncates the current ODGW exposure, which is also labeled invalid, and requires a new ODGW exposure to be started. Subsequent ODGW reads are then interleaved with reads of blocks of science image rows (i.e., ODGW interleaved-read mode) as the initial Fowler NDRs proceed.

Downloaded From: http://proceedings.spiedigitallibrary.org/ on 04/08/2013 Terms of Use: http://spiedl.org/terms

Typically, the ODGW frame rate is reduced to ~ 200 Hz in these interleaved modes. This is a compromise between maintaining high ODGW frame rate and unduly extending the science image read time, which also increases the minimum science image exposure time.

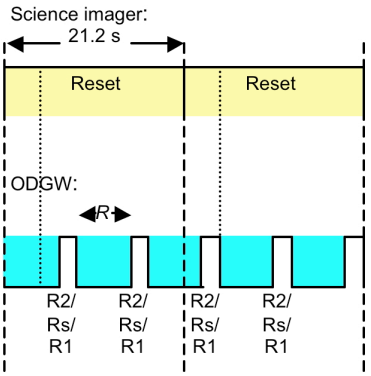

Figure 3: Science imager and fast ODGW activity during interleaved-idle operation. ODGW DCS reads (R2, Rs, R1) are separated by resets of R rows of the science imager. The science imager is reset pixel-by-pixel, so that the ODGW is not inadvertently reset.

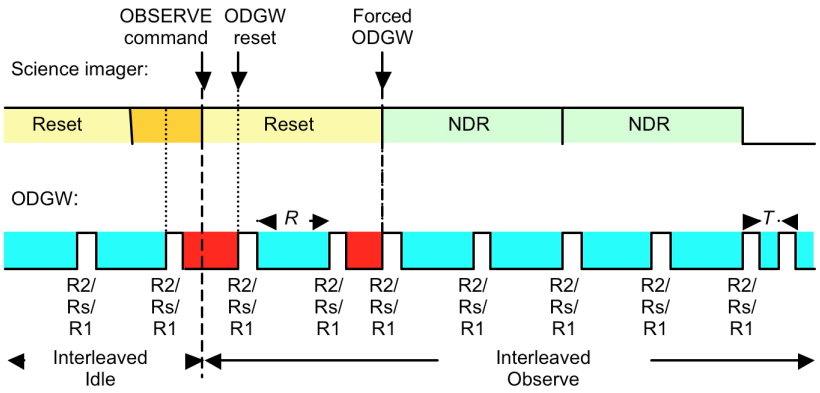

Figure 4: Science imager and fast ODGW activity during the initiation of a science imager exposure. The last interleaved-idle ODGW exposure is truncated at the OBSERVE directive (first red/dark block), again when the ODGW is asynchronously reset by the science imager reset (end of first red/dark block), and by the forced ODGW read at the start of the science imager Fowler NDRs (second red/dark block).

Once the initial NDRs are completed, the ODGW can be read out at full speed because no other science imager activity is occurring. This is when the ODGW frame rate can reach 800 Hz and the adaptive-optics correction is best. Ideally, this would be for the bulk of the science exposure time, but in practice the interval depends on how many Fowler NDRs have been requested (each Fowler NDR takes 5.3 s to execute) and the specified science exposure time.

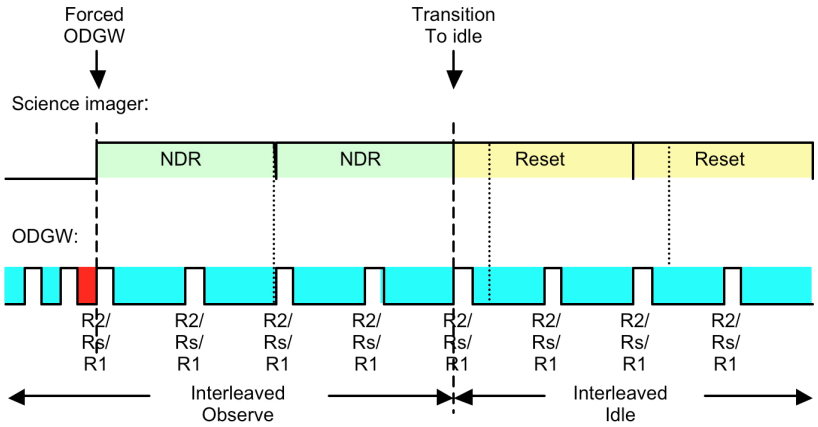

Figure 5: Science imager and fast ODGW activity during the completion of a science imager exposure. An ODGW exposure is truncated by the forced ODGW read when the final Fowler NDRs commence (red/dark block). The transition to interleaved-idle mode is seamless, as science imager resets do not reset the ODGW in interleaved-idle mode.

The science exposure ends with a second set of Fowler NDRs (Figure 5). A forced ODGW read must again occur at the start of these NDRs so that the same exposure time is maintained for all pixels. As before, this ODGW read truncates the current ODGW exposure, causing it to be restarted. The final Fowler NDRs proceed in ODGW interleaved-read mode with the ODGW frame rate throttled back to ~ 200 Hz. After the exposure has completed, the science imager reverts to its "idle" mode and the ODGW reverts to its interleaved-reset mode. At the same time, the science image data must be transferred to the Data Handling System. ODGW reads must continue uninterrupted during this data-write phase so that the adaptive-optics loops remain closed. Otherwise, time would be wasted re-closing these loops between exposures. If multiple co-added science exposures have been requested before the data are archived, the next science exposure commences immediately on the completion of the last exposure and the ODGW transitions directly to interleaved-reset

Downloaded From: http://proceedings.spiedigitallibrary.org/ on 04/08/2013 Terms of Use: http://spiedl.org/terms

mode rather than reverting to interleaved-idle mode. If multiple repeat science exposures have been requested, with each exposure archived to the Data Handling System, a new science exposure is initiated as soon as the previous image has been archived. In any event, it is necessary for ODGW reads to continue unabated, so that the adaptive-optics loops stay closed.

The ODGW frame rate is defined by a combination of two parameters (Figure 3 and Figure 4). A minimum time interval between ODGW reads, *T*, sets the minimum ODGW exposure time. This defines the frame rate (up to 800 Hz) during the mid-exposure phase when the science imager is not being read or reset. A row parameter, *R*, defines how many science imager rows are reset or read between ODGW reads during interleaved-idle, interleaved-reset, and interleaved-read operation of the ODGW. The time to process these science rows efficiently is typically longer than the exposure time, *T*, at high ODGW frame rates, so the ODGW frame rate drops in these interleaved phases.

The impact of interleaved ODGW resets and reads, and of truncated ODGW exposures, depends on the requested ODGW frame rate. When used only for flexure correction, the ODGW exposure time is typically ~ 10-30 s. Then the ODGW exposure time is typically longer than the science imager reset time (~ 5.3 s) and the time to execute initial and final Fowler NDRs. The ODGW exposure time can be selected so that truncated exposures have minimal impact on flexure monitoring. When the ODGW is operated at high frame rate for adaptive-optics correction, it is inevitable that some ODGW frames are truncated. These must be flagged as such in order to not transmit corrupted information to the adaptive-optics system. However, the effect of these missed ODGW frames is minimal because of the intrinsic self-correcting nature of the close-loop adaptive-optics operation. Of more impact is the varying ODGW frame rate in different phases of the science exposure. This requires that the ODGW be set up at frame rates of < 200 Hz, and then operated at ~ 800 Hz at mid-exposure, with correspondingly shorter ODGW exposure times.

4. SOFTWARE LAYERS

The control software for GSAOI has been implemented in a number of layers. The Gemini Observatory software components (including the GSAOI engineering screens) communicate with GSAOI using the Experimental Physics Industrial Control System (EPICS) software framework. In accordance with Gemini's conformant instrument software architecture GSAOI has implemented a software component called the Detector Controller (DC) running as an EPICS IOC on a VxWorks VME platform using a PPC7455 processor. Within the DC there are a number of distinct software modules: the DC Control module for handling incoming commands; the DC Health module for handling health and alarms; the Science Detector module (a set of tasks for dealing with science exposures); the ODGW module (a set of tasks for dealing with ODGW processing); the SDSU Device Driver (a set of tasks for interacting directly with the SDSU PCI DSP hardware); and lastly the SDSU DSP firmware itself (code that runs on the two SDSU DSP processors). These modules are depicted in the UML domain diagram of Figure 6. Figure 7 shows the EPICS engineering screen for setting the control parameters required for an ODGW guiding session – these include readout mode, exposure parameters, ODGW positions and size, output and display parameters and centroid processing parameters.

Downloaded From: http://proceedings.spiedigitallibrary.org/ on 04/08/2013 Terms of Use: http://spiedl.org/terms

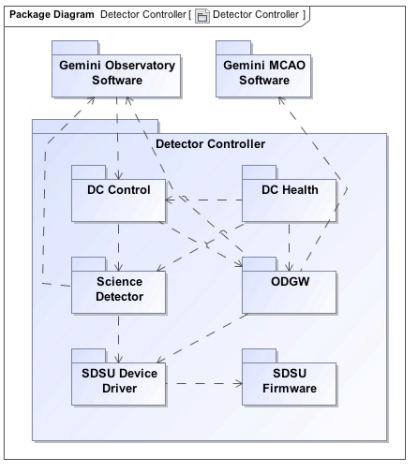

Figure 6: Software Domain diagram for GSAOI ODGW software

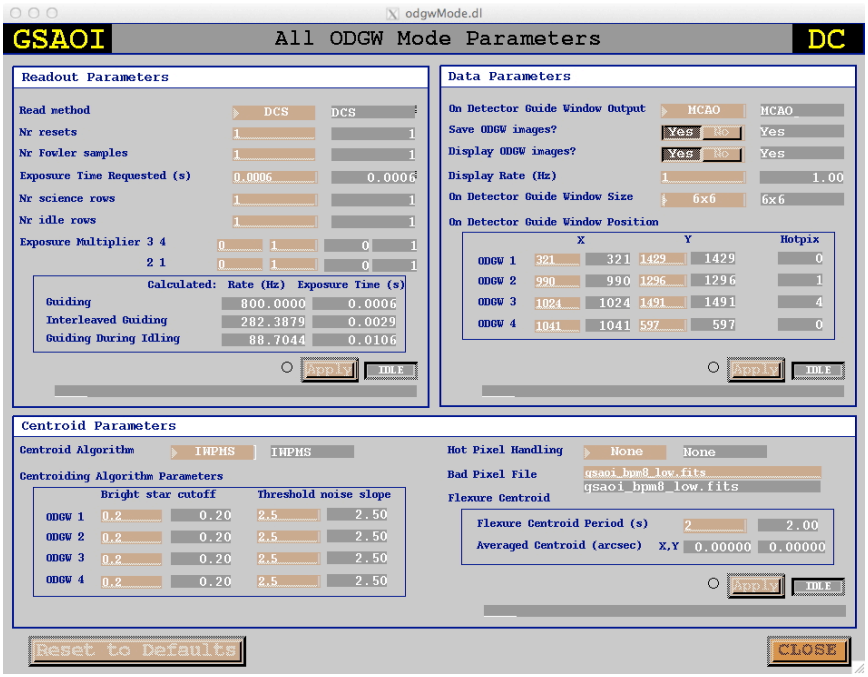

Figure 7: GSAOI ODGW control parameters

4.1 SDSU Firmware

Two DSP56300s are used by the SDSU (Astronomical Research Cameras (ARC)[1]) controller electronics for gathering the data from the GSAOI 2×2 array of H2RG detectors. The SDSU timing board Digital Signal Processor (DSP) implements the clocking patterns required for controlling the detector, receiving commands and transmitting data via a fibre-optic link to the PCI interface card in the host computer. The PCI interface board DSP manages the command interface to the host and writes received data directly into host memory via direct-memory access (DMA). GSAOI DSP code and the associated PCI device driver (§4.2) have been informed by code supplied with the purchase of SDSU electronics from ARC.

The DSP code for the GSAOI detector system was derived from the single-detector code of NIFS (McGregor et al., 2003[1]), enhanced to support reading the four GSAOI detectors through 16 output channels as well as support for ODGWs. With two independent data streams to be transmitted from the SDSU timing board DSP to the host computer PCI board DSP over a single channel, it was necessary to devise a data-packaging scheme that identified each packet as either science or ODGW data. Once data arrives at the PCI DSP it is transferred to host memory ring buffers using DMA. A host interrupt is generated after the PCI DSP processes each data packet (either science or ODGW). Each interrupt is then handled by the host interrupt service routine (ISR) by adding details of the packet to a message queue. A HI32 PCI-bus controller is used to initiate and control activity via register manipulation. The UML class diagrams in Figure 8 and Figure 9 show the relationships between the two DSPs and the host.

Reading out ODGWs is accomplished with an atomic READ2-RESET-READ1 (R2RsR1) read routine. The pixel values for both R2 and R1 are transmitted to the host computer, where a Double Correlated Sample (DCS) is obtained by subtracting R1 from the previous read from R2 from the current read. R1 and R2 can both consist of multiple Fowler samples. It is immediately clear that no time can be allowed between ODGW reads for fastest operation. The ODGW exposure time is now equal to the R1 time. For fastest operation this must be a single read, and this then results in a one-third duty cycle. Note that all DCS processing is carried out on the VxWorks PPC host, once data for R1 and R2 frames are in memory, and is triggered by a callback to the SDSU Controller module from the ISR.

[1] http://www.astro-cam.com/

Downloaded From: http://proceedings.spiedigitallibrary.org/ on 04/08/2013 Terms of Use: http://spiedl.org/terms

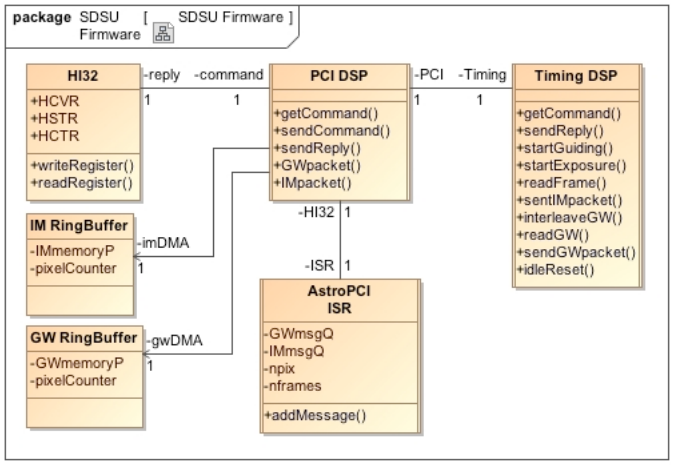

Figure 8: Class diagram for elements of the DSP firmware

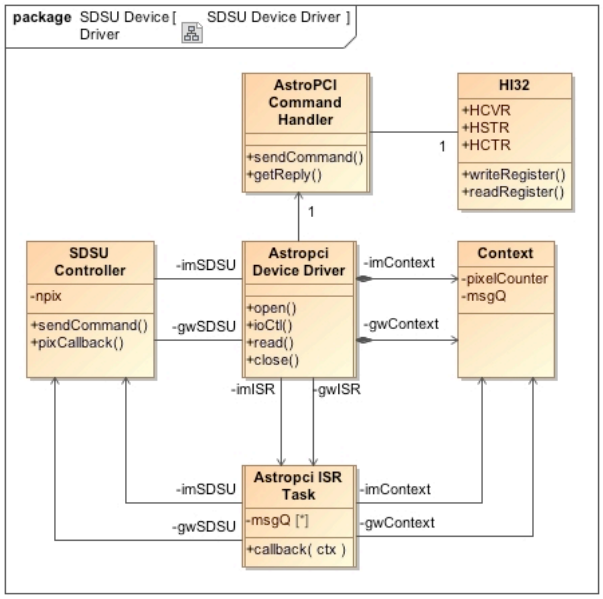

Figure 9: Class diagram representing objects in the device driver software

The situation where the only activity is the reading of guide windows is limited to the science observation exposure interval between science R1 and science R2. When a science observation is not in progress, the detectors are continuously being reset to avoid saturation. During this IDLE mode the ODGW reads must continue. ODGW reads are interleaved after *R* rows of resetting, often with *R*=1 to get a reasonable ODGW frequency. Originally the four detectors were being reset through 16 channels in parallel. This resulted in the science row resetting regularly destroying the contents of one or more ODGW reads. An ODGW avoidance scheme was devised. This necessitated that the pixels of each detector be reset serially (rather than as four quadrants in parallel), so quadrupling the reset time for the whole detector array to ~21.2s. As the clocking progresses the pixel coordinates are compared to the ODGW coordinates for each detector and the individual detector RESET_ENABLE (RsE) control signals are only asserted if the pixel in question is outside the ODGW.

The ODGWs must also be read during resetting of the science frame. Interleaving here works in a similar way to that during the IDLE phase, but because the four detectors are reset by clocking them in parallel, the ODGWs cannot be avoided and this results in corrupted ODGW information. ODGWs affected when resetting a row of science pixels are declared invalid, thus avoiding sending erroneous centroid information to GeMS.

ODGW reads need to occur at a reasonable rate during the science frame read phases as these make up a considerable fraction of the science exposure time. Again this is effected by interleaving ODGW reads between reading rows of science data. There is no danger here of corruption of ODGW data, but the RESET phase of the ODGW reads can corrupt the science reads, i.e. the bias level of the next row of science pixels to be read is disturbed, introducing artifacts in the science data. To mitigate this the science R1 and R2 are setup with exactly the same timing causing artifacts to be subtracted out in the DCS. Starting each science read phase with an ODGW read enforces this exact timing, necessarily truncating the previous ODGW cycle which is declared invalid and thus excluded from centroiding.

The resetting of the ODGW pixels does not only affect the following science pixels, but also the reading of the ODGW pixels themselves. Whether this is the result of self-heating or charge-redistribution, or a combination of the two, is still a matter of discussion, but a combination of resetting with READ_ENABLE (ReE) active and exercising the column buffers by dummy reading the first row removes the disturbance of the science read-out by the preceding science reset. For ODGWs the time between Rs and R1 is not long enough to have the reset disturbance settle. This results in a slope on the ODGW background that induces an offset in the centroiding of the guide star. The centroiding algorithm has been optimized to remove this slope.

Downloaded From: http://proceedings.spiedigitallibrary.org/ on 04/08/2013 Terms of Use: http://spiedl.org/terms

Each ODGW is restricted to have the same size and shape (which, for convenience, is square). Although any size can be programmed in the detector multiplexer and the detector controller, only 2×2, 4×4, 6×6, 8×8, 10×10, 16×16, 24×24, 32×32, 64×64 and 128×128 have been implemented in the host computer software.

The brightness of available guide stars can vary considerably, necessitating different ODGW exposure times for one or more of the guide windows. This is implemented through the use of "Guide Window Exposure Multipliers". A suitable exposure time is chosen for the ODGW with the brightest guide star, while the other ODGW exposures are set to multiples of this value. The Rs phase of the R2-Rs-R1 cycle is replaced by a dummy Rs - by turning the RsE signal off for the detectors with the longer ODGW exposures. The read data are discarded. Only at the end of an exposure is the usual reset applied and the read data used.

4.2 VxWorks device driver

Shown in Figure 9 are three active classes comprising the Astropci (SDSU) device driver – the "Device Driver" (with the standard VxWorks driver API implemented), the "Command Handler" (for sending/monitoring commands to the PCI DSP and handling replies) and the "ISR task" (for consuming packet messages placed on a queue by the ISR – and then issuing a callback to the higher level "SDSU Controller" module for it to update its bookkeeping and initiate DCS processing). The design of this driver is such that it minimizes any delay in triggering required processing of the ODGW and science image frames once they arrive. The multi-threaded design of the code also ensures that any new incoming commands (for example to abort, stop or pause guiding) are processed in a timely fashion.

The device driver also supports full simulation mode where realistic GSAOI science and ODGW data are generated artificially. In the case of ODGW data, fake stars are constructed using Gaussian star profiles that move around randomly.

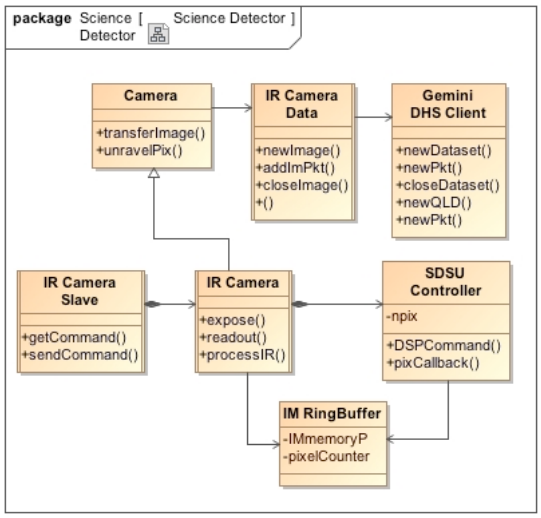

Figure 10: Class diagram for the science detector

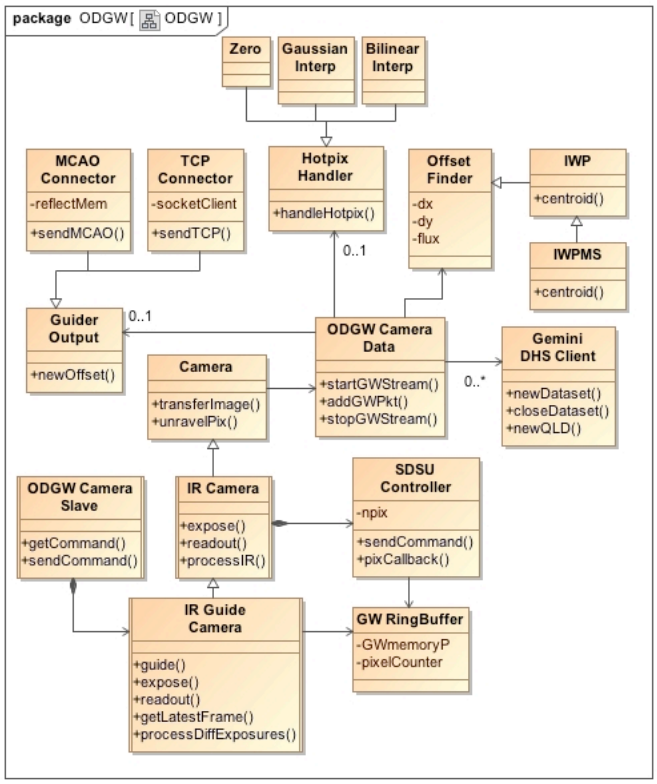

Figure 11: Class diagram for the ODGW software

4.3 VxWorks host high-level software

Figure 10 and Figure 11 show the high-level host classes that handle the pixel data once they arrive in the host ring buffers. Separate VxWorks tasks handle data from each of the science and ODGW data streams.

Downloaded From: http://proceedings.spiedigitallibrary.org/ on 04/08/2013 Terms of Use: http://spiedl.org/terms

4.3.1 IR Camera module – IR data processing

For the science data stream the "IR Camera" class processes pixels as they arrive in a parallel fashion, i.e. DCS processing is started as soon as a significant chunk of data arrives and then data are unraveled from the interleaved pixel stream on an amplifier basis (there are four readout amplifiers per H2RG – making sixteen in all) and then transferred ("IR Camera Data" & "Gemini DHS Client" classes) to the Gemini DHS for storage and quick-look display. This parallel architecture reduces the duty cycle for taking science exposures to a minimum. The UML sequence diagram of Figure 12 gives an indication of the chain of events in the exposure sequence. Note that there are many software objects involved in this complex sequence from initiation of the "Observe" command by the operator of the Gemini engineering GUI until the data are dispatched to the Gemini DHS. This acquisition design was reported previously, in more detail, by Young (2008)[5].

For the ODGWs, the processing sequence is somewhat similar in that each ODGW frame needs to have infrared processing performed and pixels unraveled (they are delivered as an interleaved stream from the four ODGWs). In addition to this "standard" work, each frame needs to be cleaned of hot pixels and centroided with the data then transmitted to the GeMS system as well as to the DHS (see Figure 11).

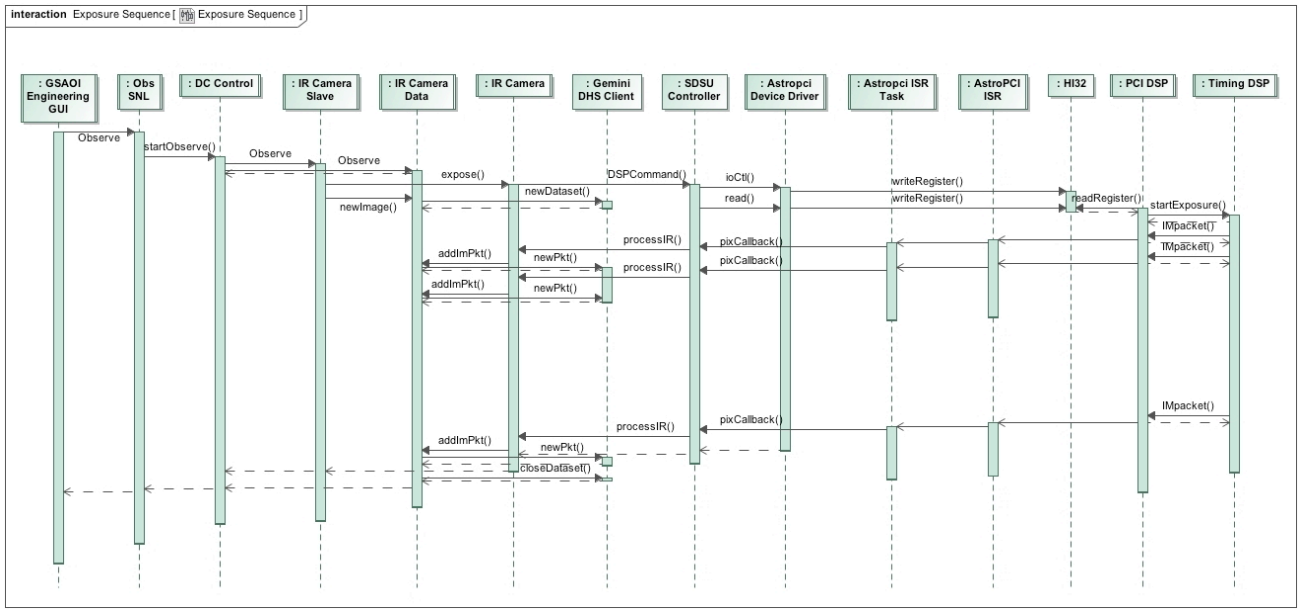

Figure 12: Partial sequence diagram showing complex events during a science exposure sequence.

4.3.2 Data quality checks – R1 or R2, validity and latest frame detection

As the GSAOI DC has been implemented on a uni-processor single board computer there is obviously competition for the CPU resource amongst the set of concurrently executing tasks. Because the ODGW processing should be completed with minimal latency so as to deliver centroid information to GeMS in close to real-time, it has been necessary to tune the VxWorks runtime priorities of critical ODGW related tasks. Inevitably, under some high load conditions (e.g. running small (2x2) ODGWs as fast as possible – i.e. with minimum exposure time), ODGW frames sometimes build up in the "GW RingBuffer" – meaning older frames have stale information and therefore should be discarded.

A recursive algorithm has been developed to search ahead in the "GW RingBuffer" to find the latest ODGW frame for processing. This is more complicated than it seems at first – given that the system has been designed to support ODGWs with variable exposure times. The lookup procedure needs to ensure that chosen ODGWs are in phase – this is illustrated by the example of Figure 13– the "Pptr" label indicates where in the ring processing has reached, while the "Tptr" label shows that latest data delivered to the ring. Note that ODGW1 is one frame ahead of ODGW2 - which has twice the exposure time. Data packets "A" and "B" are chosen for processing as they are in phase. Statistics are kept of how many frames are skipped with associated details – these can be inspected later to monitor the performance of the system.

Downloaded From: http://proceedings.spiedigitallibrary.org/ on 04/08/2013 Terms of Use: http://spiedl.org/terms

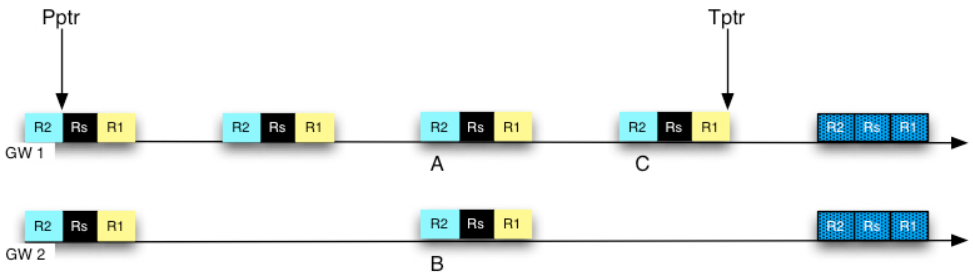

Figure 13: Timeline of ODGWs with different exposure times - latest data from ODGW1 is ahead of latest data from ODGW2. Choose A & B for processing as they are in phase.

The ODGW processing algorithm also needs to consider whether or not a frame ready for processing is valid. Recall how during ODGW clocking some frames may get marked as invalid due to a disruption of the processing sequence when transitioning across exposure phases or during full-frame resetting (see §4.1) – these frames are ignored with no centroiding calculations performed. Each ODGW frame in the ring buffer has a companion header structure with flags indicating frame type (whether R1, R2), validity and reset status.

4.3.3 Performance enhancements - use of Altivec

A technique chosen to reduce the ODGW centroid latency caused by the infrared processing is to use the PowerPC's in-built Altivec engine. Altivec is a 128 bit vector processing unit that enables up to four 32-bit calculations to be performed simultaneously – ideally suited to the processing of pixel data. In reality, due to overheads in setup of the vector registers and data pipeline synchronization, we have found that maximum speedups of about 3.5x are possible for some operations (division operations show greatest gains). However, the use of Altivec is sensitive to the number of pixels being processed in each operation with experimentation showing that a buffer size of 128 is the break-even cutoff. An operation with less than 128 pixels actually results in increased CPU usage, so Altivec is conditionally only used when buffers are larger.

4.3.4 Centroiding Algorithms

The centroiding algorithm used is based on the usual center-of-mass - or intensity-weighted position (IWP), algorithm with added pixel thresholding. Thresholds are applied to first cut outliers in the intensity distribution (typically 15%) and then to eliminate frames that do not reach a minimum flux. The flux threshold is calculated using an exponential function of the RMS noise (standard deviation) devised by Gemini for their general-purpose wave front sensors (Boyer, 2003[8]). The pixel threshold is set to be $\mu+m\sigma$ where m is set to 2.5 by default (μ is the mean pixel intensity for non-outlying pixels, σ is the standard deviation).

As mentioned in §4.1, the image anomaly caused by an ODGW reset and delayed settling time causes a ramp across each ODGW frame – affecting the IWP centroid algorithm. To remove this effect, it was necessary to devise a modification to the IWP calculation such that this image ramp is removed. A number of border pixels are used to calculate the x & y slopes across each image that are then used to remove the ramp from each pixel in the core of the frame – see Equation (1) where x, y are the pixel coordinate, w, h frame width and height and xs, ys the x & y slopes.

$$p' = p - ((x - w/2) * xs + (y - h/2) * ys) \quad (1)$$

4.3.5 Interface to GeMS system via reflective memory, synchronization scheme

GSAOI transfers ODGW frame data to GeMS via the Gemini Synchro Bus. The Synchro Bus is implemented as a reflective memory ring with nodes on the ring 'owning' a dedicated 1KB page of the shared reflective memory – this is described in detail in Gemini ICD 10[2]. Each ODGW packet put on the bus consists of tip, tilt, flux, time-stamp (international atomic time (TAI) from the Gemini time bus[3]), update counter (one for each ODGW - incremented each new update), a mask that indicates which ODGWs are valid and two synchronization counters – one at each end of the packet. Updating the first synchronization counter at the beginning of a new write and then updating the second counter at the end of a write achieves synchronization. The reader (GeMS) reads the whole block and checks that both counters

[2] http://www.gemini.edu/documentation/webdocs/icd/icd_10.pdf
[3] http://www.gemini.edu/documentation/webdocs/icd/icd_09.pdf

Downloaded From: http://proceedings.spiedigitallibrary.org/ on 04/08/2013 Terms of Use: http://spiedl.org/terms

are equal to ensure validity. Note that GeMS needs to sample the reflective memory fast enough to ensure updates are gathered without increasing end-to-end latency by a significant amount.

At the time of writing, the GeMS RTC cannot use the TAI time-stamps because the TigerSHARC DSP processor used for performing the RTC computations does not support the double floating point type. We are currently investigating an alternative way of providing this information – perhaps by using single precision time-stamps, given the required resolution is only 1.25ms (i.e. to support the fastest guiding rate of 800Hz).

4.3.6 Hot pixel handling

Because the GSAOI H2RG detectors have many hot pixels (pixels glow at intensities higher than background RMS noise values – with intensity non-linearly related to exposure time), methods of removing their effect have had to be devised. Evaluation of a few techniques for accuracy and computation time has been performed – with, as one would expect, higher accuracy achieved with methods that require longer computation:

- Zero out hot pixels
  Simply replacing hot pixels with zero values improves centroid accuracy significantly and can be done quickly (this effectively removes these pixels from the IWP centroid calculation).
- Bilinear interpolation
  Each hot pixel is replaced with the average of the weighted sum of surrounding pixels going out to a radius *r*.

$$p_{x,y} = \sum_{i=x-r,j=y-r}^{i=x+r,j=y+r} p_{i,j} w_{i,j} \Bigg/ \sum_{i=x-r,j=y-r}^{i=x+r,j=y+r} w_{i,j}, w_{i,j} = 1/\sqrt{(x-i)^2 + (y-j)^2} \quad (2)$$

  This algorithm produces reasonably accurate results in most circumstances. Of course, if a hot pixel coincides with the centroid the profile will be flattened. It is also quite fast. Setting the radius $r = 1$ gives a more accurate result compared to $r = 2$ for the samples chosen.
- Elliptical Gaussian interpolation
  The elliptical Gaussian algorithm should fit a more realistic distribution to the data, but the computation required is considerably longer. The numerical implementation of an elliptical Gaussian fit to the data is well described elsewhere[4] and will not be repeated here.

To accurately assess the performance of each algorithm, guide stars were simulated using a simple circular Gaussian with random Gaussian noise added to represent a "background" level. These stars were then moved around in a random fashion to simulate atmospheric turbulence in a simple fashion. Hot pixels were then added to each GW according to the real GSAOI bad pixel mask generated by detecting all the hot pixels from a GSAOI dark frame. Each algorithm was used to replace the hot pixels with an interpolated value and a centroid calculation performed. This was then compared with the known centroid location. Table 1 shows the results obtained.

Table 1: Hot pixel interpolation results. Simulations run with four 8×8 ODGWs and with 10, 5, 2, 2 hot pixels in each ODGW respectively. Guide stars simulated using circular Gaussian with random Gaussian noise added across image.

Algorithm	N	Avg Error (pix)	Avg Error #hotpix<=5 (pix)	Avg time (s)
None	10085	0.761	0.476	1.15E-05
Zero	10065	0.158	0.059	1.07E-05
Bilinear (*r*=1)	10022	0.098	0.057	1.84E-05
Bilinear (*r*=2)	10069	0.117	0.072	2.99E-05
Gaussian	10055	0.049	0.032	9.98E-04

[4] http://en.wikipedia.org/wiki/Gaussian_function

Downloaded From: http://proceedings.spiedigitallibrary.org/ on 04/08/2013 Terms of Use: http://spiedl.org/terms

4.3.7 DHS interface and data recording

The Gemini DHS is used for recording ODGW data – both for display and analysis. Communications with the DHS is by way of the Gemini data LAN (fast Ethernet), meaning that it is not a high performance system. It has been identified as a considerable bottleneck in the time required for a full GSAOI observation cycle. For ODGWs saving/displaying image frames as soon as they are produced is impossible. To overcome this, ODGW data frames are buffered on the GSAOI DC IOC and delivered to the DHS using the "DHS Client" module at the end of a guiding session. In addition, frames are sampled at a much lower rate (typically 1-5 Hz) and sent to the DHS for real-time display, so that a live indication of what is being acquired can be provided.

As mentioned earlier, the GSAOI DC is CPU performance challenged with the processing required for science and ODGW data. ODGW throughput can be thus affected if attempting to display ODGW data frames at too high a rate – especially when guiding fast using small ODGWs. Operationally, a compromise between what is a useful rate for display and ODGW throughput has been found.

The ODGW data frames saved at the end of a run are organized into a continuous strip of the four ODGWs arranged in a 2×2 array. Along with pixel data, other data including time-stamp, tip-tilt and flux values are saved for later analysis and correlation.

4.3.8 Abort handling

During the operation of GSAOI, changing the run-mode of the instrument is a common occurrence. For example, modifying an ODGW operational parameter requires that the current guiding session be aborted and restarted with the new parameter.

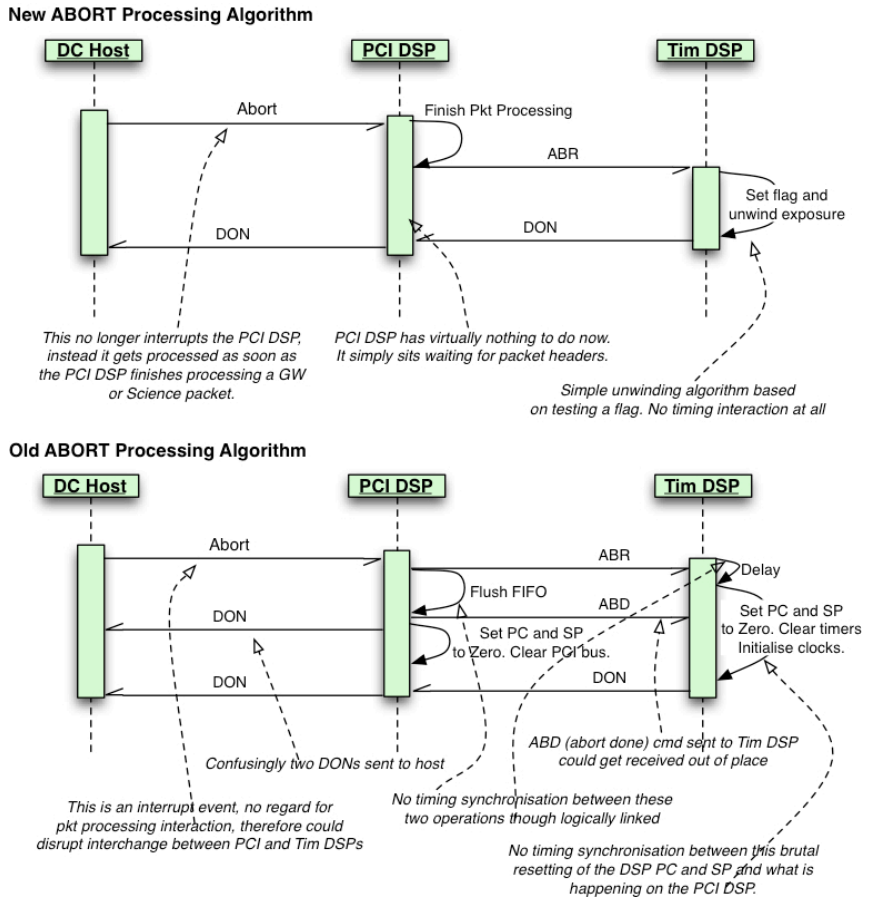

Figure 14: SDSU DSP Abort algorithm improvement. Original (bottom) SDSU DSP code had a complicated Abort algorithm that was not robust to failure. Simpler refinement of this algorithm (top) ensured robustness and met frequent use requirement of GSAOI.

Downloaded From: http://proceedings.spiedigitallibrary.org/ on 04/08/2013 Terms of Use: http://spiedl.org/terms

As detailed earlier, the processing architecture for GSAOI is quite complex – so aborting a guiding session (or aborting a science exposure) is also complex. Getting this working robustly for GSAOI has been a challenge – in particular on the SDSU DSPs. The original SDSU DSP code did not handle aborts well. This was modified as shown in Figure 14 so that the algorithm is simpler and has proven to be very robust.

4.4 GeMS RTC

Figure 15 shows the data flow between GSAOI and the GeMS Real Time Controller (RTC) in more detail.

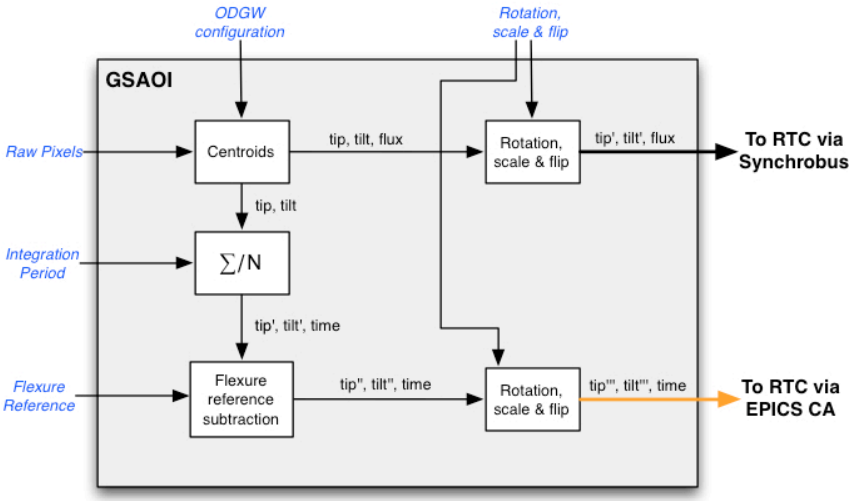

Figure 15: GSAOI to GeMS data flow detail (courtesy C. Boyer, Gemini Observatory, 2006)

4.4.1 Tip-Tilt processing

Tip tilt values from GSAOI are sent to the GeMS RTC via a reflective memory path. The three NGSs provide the six X-Y slopes that are necessary for generating global tip and tilt residuals and plate-scale modes. Tip and tilt are derived from the average of the X-Y slopes. Plate-scale modes are derived using combinations of quadratic modes (Ellerbroek & Rigaut, 2001[6]). The tip-tilt residuals and plate-scale modes are computed by a task running on the RTC. This loop can be closed at a rate of up to 800Hz.

4.4.2 Flexure centroid processing

The flexure signals are sent via an EPICS channel because the loop rate requirement is low. Flexure updates can be sent at a rate of as low as 0.1 Hz and up to 30 Hz. First results obtained on-sky have shown that the differential flexures between the adaptive optics optical bench and GSAOI are small: of the order of ~ 0.2 arcsec on-sky for 30 degree elevation steps.

The flexure signal is used as soon as the tip-tilt loop is closed, by moving the three tip-tilt WFS probes all together. As the tip-tilt loop is closed on the signal coming from these probes, moving the probes moves the tip-tilt mirror accordingly, and results in an image motion at the science detector level.

4.5 Support for ODGWs in the Gemini high-level software

Control of the GSAOI ODGW operation has been integrated into the Gemini Observatory high-level software. Depending on the NGS magnitude, the ODGW exposure time, (and therefore, the number of interleaved rows for each operating mode) is set automatically. The location of the ODGW on the science detector is set using NGS sky coordinates based on star catalog positions. A linear translation matrix is used to map the on-sky coordinates to x-y pixels in the science frame. To facilitate acquisition of the NGS, the operator usually starts with a large ODGW size (64×64 or 128×128) and then re-centers the star in the window. Once centered, the size of the ODGW is reduced to the best compromise between frame rate and exposure time, while optimizing the signal-to-noise ratio. Depending on the GSAOI filter used, an offset is applied to the location of the ODGWs to take into account filter wedge effects. These offsets have been measured and calibrated using Canopus internal reference sources. For example with the H-filter, these

Downloaded From: http://proceedings.spiedigitallibrary.org/ on 04/08/2013 Terms of Use: http://spiedl.org/terms

offsets are of the order of 0.5 pixels, growing to as large as 4 pixels for some narrow band filters (Br gamma, CO, Kl-continuum).

5. RESULTS

5.1 Laboratory performance

Both flexure and fast tip-tilt loops have been characterized using the internal calibration sources in Canopus. Figure 16 shows a K-band image of the calibration sources for the four 32×32 ODGWs (each of the calibration stars has a different flux used for characterizing signal-to-noise ratio performance).

The internal sources have been used extensively to characterize the performance of the fast tip-tilt loop. Figure 17 shows a measurement of the ODGW frame rates obtained across the full science exposure cycle (idle, interleaved and guiding). Figure 18 shows a zoomed in plot of the sharp transition from interleaved guiding to the pure guiding segment running at 800 Hz. The ODGW settings for this example were those as shown in Figure 7 with a 30 s science exposure time.

To characterize the ODGW closed loop, the error transfer function (ETF) of the tip-tilt loop has been measured. Following a simple procedure, the open-loop and closed-loop centroids were recorded while operating under noise-only conditions. The ETF was then computed by normalizing the closed-loop transfer functions with the open-loop ones. The measurements were repeated for different loop gains (between 0.1 to 1.0) and different loop rates (from 100 Hz to 800 Hz). Finally, we fitted the ETF with a simple model that takes into account the delays in the loop.

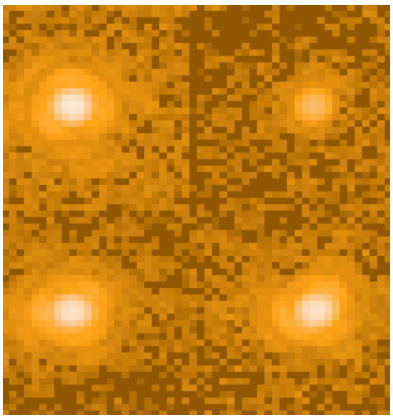

Figure 16: K-Band ODGW.

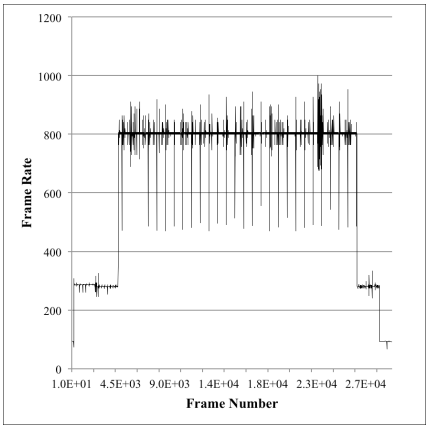

Figure 17: ODGW frame rate (Hz) – full cycle.

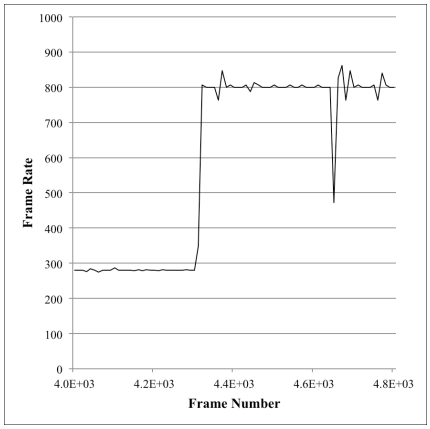

Figure 18: ODGW frame rate (Hz) – transition from interleaved to 800Hz region.

Figure 19 shows the ETF obtained for the X-axis (tip measurement - at 280 Hz, gains of 0.5 and 1.0). The bandwidth achieved is around 20 Hz, which is in good agreement with the performance obtained when using the Canopus visible tip-tilt WFS.

Downloaded From: http://proceedings.spiedigitallibrary.org/ on 04/08/2013 Terms of Use: http://spiedl.org/terms

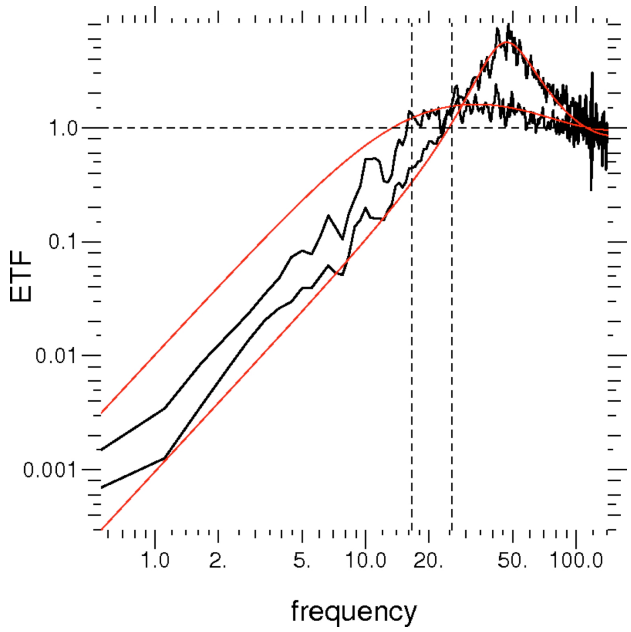

Figure 19: ODGW error transfer function (black=measured, red smooth=theoretical).

5.2 On-Sky results

The flexure compensation loop has been successfully closed on-sky, and it is now fully integrated into GeMS regular operations. The fast tip-tilt guiding has not yet been fully tested on-sky, but preliminary work on limiting magnitude and centroid accuracy for different signal-to-noise ratios is on going. Figure 20 shows an example of four images obtained with the K-short filter, on a K=10.3 mag star, for 10 ms exposure time (frame rate = 7 Hz). The signal-to-noise ratio (defined as the maximum divided by the RMS of the background) was approximately 150. The fifth image in Figure 20 is a 1.6 ms exposure of the same star where the signal-to-noise ratio reduces to around 2.5, but still good enough to provide a centroid accuracy of 0.1 pixel.

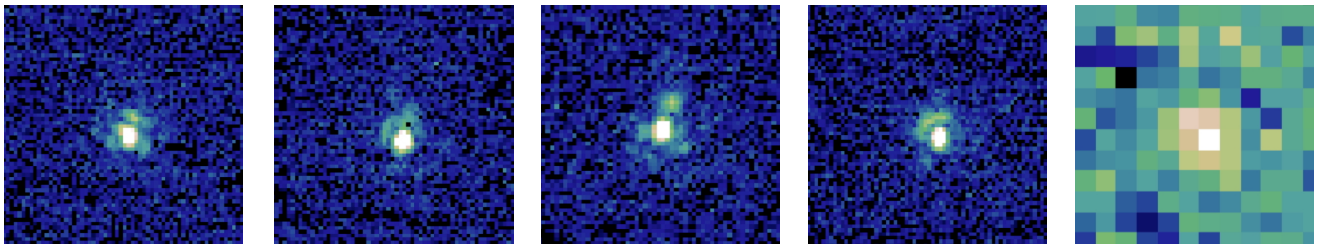

Figure 20: K-short band ODGW images, first four 10ms exposure, fifth 1.6ms exposure

6. CONCLUSIONS

In addition to providing tip-tilt information, we believe that the ODGW capability of GSAOI can provide a very powerful tool for performance evaluation and optimization. Indeed, the ODGWs provide a real-time image of what is happening directly on the science detector, which is where one wants to optimize performance. This is a unique capability, which could provide on-line performance optimization, vibration characterization and non-common-path aberration control (ODGWs can be used as a truth sensor). These optimizations are currently being undertaken manually, but we plan to automate the procedure, in order to maximize GSAOI performance. ODGWs also provide unique and valuable input for point spread function estimation and reconstruction, providing a set of short-exposure images in different locations over the field. In addition, in the case of GeMS, we are investigating the possibility of using the ODGWs as a focus sensor, based on the new development around focal plane WFS (Plantet, 2012[7]). Finally, ODGWs can also be used as a numerical coronagraph, to avoid bright star saturation in the field, and enhanced signal in

Downloaded From: http://proceedings.spiedigitallibrary.org/ on 04/08/2013 Terms of Use: http://spiedl.org/terms

surrounding bright stars. In a good performance regime, the stars have a full width half maximum (FWHM) of roughly two pixels, which is the size of the smallest ODGW.

In summary, we believe that this ODGW capability opens a very versatile area for performance characterization and optimization, which is unique. The main drawback though is that as the ODGW are located on the science array, the flux received will be filter dependent, and the use of the ODGW in fast mode may be limited to just broad-band filters.

Implementing the requirements for support of ODGWs in the GSAOI software system has taken a considerable effort. This effort is currently being rewarded with the promising results obtained during commissioning and presented here. The Gemini Observatory looks forward to being able to offer the GSAOI instrument with its adaptive optics capability as an available resource for the Gemini community in the near future.

REFERENCES

[1] McGregor, P., Hart, J., Conroy, P.G., Pfitzner, M.L., Bloxham, G., Jones, D.J., Downing, M.D., Dawson, M., Young, P. and Jarnyk, M., van Harmelen, J. "Gemini near-infrared integral field spectrograph (NIFS)", Proc. SPIE 4841, (2003).

[2] McGregor, P., Hart, J., Stevanovic, D., Bloxham, G., Jones, D., van Harmelen, J., Griesbach, J., Dawson, M., Young, P. and Jarnyk, M. "Gemini South Adaptive Optics Imager (GSAOI)", Proc. SPIE 5492, (2004).

[3] Neichel, B., Rigaut, F., Bec, M., Boccas, M., Daruich, F., D'Orgeville, C., Fesquet, V., Galvez, R., Garcia-Rissmann, A., Gausachs, G., Lombini, M., Perez, G., Trancho, G., Upadhya, V. and Vucina, T. "The Gemini MCAO System GeMS: Nearing the End of a Lab-Story", Proc. SPIE vol. 7736, no. 773606 (2010).

[4] Rigaut, F. and Neichel B. "Gemini South MCAO on-sky results", 2nd AO4ELT Conference, Victoria, Canada, 25-30 Sept., 2011.

[5] Young, P.J., Nielsen, J., Roberts, W.H. and Wilson, G.M. "Achieving Design Reuse: a Case Study", Proc. SPIE Volume 7019, pp. 70192M-70192M-12 (2008).

[6] Ellerbroek, B.L. and Rigaut, F. "Methods for correcting tilt anisoplanatism in laser-guide-star-based multiconjugate adaptive optics", J. Opt. Soc. Am. A, 18, 2539-2547 (2001).

[7] Plantet, C., Meimon, S.C., Conan, J.M. and Fusco, T. "LIFT - a noise-effective low order focal-plane sensor: from theory to full experimental validation" SPIE Astronomical Telescopes + Instrumentation, Paper 8447-60, (2012)

[8] Boyer, C. "Gemini WFS Algorithms, V2.0" Internal Gemini Observatory document, (2003).

Downloaded From: http://proceedings.spiedigitallibrary.org/ on 04/08/2013 Terms of Use: http://spiedl.org/terms